

Post-Planck Dark Energy Constraints

Dhiraj Kumar Hazra^a Subhabrata Majumdar^b Supratik Pal^c Sudhakar Panda^d Anjan A. Sen^e

^aAsia Pacific Center for Theoretical Physics, Pohang, Gyeongbuk 790-784, Korea

^bTata Institute for Fundamental Research, Mumbai, 400005, India

^cPhysics and Applied Mathematics Unit, Indian Statistical Institute, Kolkata, 700108, India

^dHarish Chandra Research Institute, Allahabad, 211019, India

^eCenter For Theoretical Physics, Jamia Millia Islamia, New Delhi-110025, India

E-mail: dhiraj@apctp.org, subha@tifr.res.in, supratik@isical.ac.in,
panda@mri.ernet.in, aasen@jmi.ac.in

Abstract. We constrain plausible dark energy models, parametrized by multiple candidate equation of state, using the recently published Cosmic Microwave Background (CMB) temperature anisotropy data from Planck together with the WMAP-9 low- ℓ polarization data and data from low redshift surveys. To circumvent the limitations of any particular equation of state towards describing all existing dark energy models, we work with three different equation of state covering a broader class of dark energy models and, hence, provide more robust and generic constraints on the dark energy properties. We show that a clear tension exists between dark energy constraints from CMB and non-CMB observations when one allows for dark energy models having both phantom and non-phantom behavior; while CMB is more favorable to phantom models, the low- z data prefers model with behavior close to a Cosmological Constant. Further, we reconstruct the equation of state of dark energy as a function of redshift using the results from combined CMB and non-CMB data and find that Cosmological Constant lies outside the 1σ band for multiple dark energy models allowing phantom behavior. A considerable fine tuning is needed to keep models with strict non-phantom history inside 2σ allowed range. This result might motivate one to construct phantom models of dark energy, which is achievable in the presence of higher derivative operators as in string theory. However, disallowing phantom behavior, based *only* on strong theoretical prior, leads to both CMB and non-CMB datasets agree on the nature of dark energy, with the mean equation of state being very close to the Cosmological Constant. Finally, to illustrate the impact of additional dark energy parameters on other cosmological parameters, we provide the cosmological parameter constraints for the “Standard Model of Cosmology” including an evolving dark energy component, for the different dark energy models.

Contents

1	Introduction	1
2	Dark Energy Parametrizations	4
2.1	CPL Parametrization	4
2.2	SS Parametrization	4
2.3	GCG Parametrization	5
3	Methodology	6
4	Results	7
5	Conclusions	15

1 Introduction

It is now established beyond doubt by a range of cosmological observations, that our universe is going through a late time accelerated expansion phase. To explain such an accelerating universe, one either needs to add an additional exotic component, called dark energy, in the energy budget of the universe that necessarily has a negative pressure causing an overall repulsive behavior of gravity at large cosmological scales (see [1] for some excellent reviews), or one has to modify Einstein’s General Relativity. Unfortunately, while candidates for dark energy have been proposed, its exact nature remains unknown. Alternatively, satisfactory modifications of General Relativity consistent with gravitational physics at astrophysical scales are also lacking.

Tight observational evidence is still lacking as to whether dark energy, where one has to add an extra component in the energy budget, has a constant energy density throughout the history of the universe (termed as Cosmological Constant), or if it evolves in time. Specifically, if it evolves, one would like to know its equation of state which governs this evolution. One would also like to know if this equation of state satisfies the weak energy condition such that it dilutes with the cosmological expansion. Moreover whether dark energy violates the weak energy condition and behaves like some mysterious form of phantom energy with its energy density increasing with time and possibly leading to a future singularity is also discussed widely in literatures.

The majority of the current and future cosmological observational programs are dedicated to finding answers to these pertinent questions. These include, among others, (i) the construction of the Hubble diagram using Supernova Type-Ia as standard candle [2], (ii) measuring the tiny fluctuations present in the temperature of the cosmic microwave background radiation [3, 4], or (iii) measuring the oscillations present in the matter power spectrum through large scale structure surveys [5].

The simplest example for dark energy is the Cosmological Constant (Λ). The concordance Λ CDM model is consistent with most of the cosmological observations.

However, deep theoretical issues such as fine tuning as well as cosmic coincidence problems have motivated people to explore beyond the Cosmological Constant, the natural alternatives being scalar field models. A variety of such scalar field models, including string theory embeddings for a positive Cosmological Constant [6], quintessence [7], k-essence [8], phantom fields [9], tachyons [10] etc have been proposed. Other than scalar field models, a barotropic fluid with an equation of state $p(\rho)$, such as the Generalized Chaplygin Gas (GCG) and its various generalizations [11, 12] have also been considered for dark energy model building.

Since current cosmological observations provide us a precise description of the universe and impose tight constraints on the standard cosmological model, the general behavior of the dark energy component is also constrained. On the other hand, given the proliferation of dark energy models in the literature, it is not practical to confront each model with the observational data. Rather one needs to look for generic features of dark energy that are present in a large class of models and then to confront these features with the observational results. The most popular way of doing this is to assume a parametrization for the dark energy equation of state w as a function of redshift, z , or the scale factor, a . However, such parametrization should describe a wide variety of dark energy models so that by constraining a minimal set of parameters, one can constrain a large set of representative dark energy models. One such widely used parametrization is the Chevallier-Polarski-Linder (CPL) parametrization first discussed by Chevallier and Polarski [13] and later by Linder [14]. It uses a linear dependence of the equation of state on the scale factor and contains two parameters. This parametrization has been used by all recent cosmological observations, including Planck, to put constraints on dark energy. However, since the CPL parametrization has the dark energy equation of state as a linear dependence on a , it may not represent models with more complicated a dependence at slightly higher redshifts where dark energy contribution might still be non-negligible. Hence, constraining dark energy behavior using *only* the CPL parametrization might give biased, or even incorrect, conclusions.

Given the fact that Planck [4], in combination with non-CMB observations like SN-Ia, BAO, HST etc, has measured the cosmological content of the universe with unprecedented accuracy, it is now interesting to investigate how different parametrizations of dark energy equation-of-state can result in different constraints on dark energy behavior when confronted with the observational data. We can, now, ask the following questions - Are conclusions regarding the nature of dark energy borne out of observational data biased by our choice of parametrization? Or does a general pattern exist in the dark energy behavior that is always true even if we consider different parametrizations for dark energy equation of state?

In this paper, we investigate these issues by considering two more parametrizations for the dark energy equation of state together with the CPL parametrization. The first of the two parametrizations used in this paper was proposed by Scherrer and Sen (SS) [15] and it represents slow-roll thawing class of canonical scalar field models having an equation of state which varies very close to the $w = -1$ irrespective of the form of the potential. Subsequently, the idea was also extended to phantom type scalar field models with a negative kinetic energy term [16] where it was shown the parametrization

holds true also for such scalar field models. Recently, it was also shown [17] that this parametrization can represent scalar field models with DBI type kinetic energy term under similar slow-roll conditions.

The second parametrization which we consider, was proposed by Bento, Bertolami and Sen [11] and subsequently was discussed [19–22] for more general parameter ranges by Scherrer and Sen [12] and is known as Generalized Chaplygin Gas (GCG) parametrization. In this parametrization, for a certain choice of parameter range, the dark energy equation of state behaves like a thawing class of scalar field models where the present acceleration is a transient one. For a different choice of parameter range, the parametrization represents the freezing/tracker type models. Hence with a single equation of state parametrization, one can model both the thawing as well as freezing class of scalar field models. Recently, this parametrization has been used [23] to study the Bayesian Evidence for thawing/freezing class of the dark energy models using different observational results including WMAP-7 results.

For all of the three parametrizations, we reconstruct the redshift evolution of the dark energy equation of state. For each case, we also investigate the departure of the cosmological parameters from the Λ CDM best-fit values. Note, that the CPL parametrization has already been discussed in the Planck analysis [32]. However our analysis, apart from showing a consistency check with Planck results, provides some new facts and highlights a tension between CMB and non-CMB observations. Using the CMB, non-CMB and combined data of both, we show a clear tension between high-redshift and low redshift measurements for models allowing phantom behavior. Moreover from the combined analysis, using the correlation between the equation of state parameters we reconstruct the allowed range of dark energy evolution with redshift and address the stand of phantom and non-phantom models in the allowed band. In particular, we show that once we allow phantom behavior, the allowed non-phantom behavior is extremely close to the Cosmological Constant, $w = -1$, behavior.

At this point it should be noted that, as an alternative approach, model independent reconstructions of the expansion history (*i.e.* the Hubble parameter $h(z)$) have been carried out before [24, 25], from which the equation of state can also be reconstructed. Also note that certain parametrization of the dark energy equation of state may ‘artificially’ limit the properties of dark energy from explaining a few effects, such as the recent slowdown of cosmic acceleration [26]. To overcome such biases, in this current work, we use three different kinds of dark energy parametrizations in order to cover a broad spectrum of dark energy behavior. We constrain the nature of dark energy using CMB and non-CMB surveys, taken individually as well as jointly (see [27] for some recent works on dark energy constraint after Planck).

The paper is organized as follows: in Section 2, we briefly describe the three dark energy parametrizations that we use in this paper; in Section 3, we describe the different observational datasets that we use to constrain the dark energy evolution; Section 4 describes the results and we conclude in Section 5.

2 Dark Energy Parametrizations

2.1 CPL Parametrization

This parametrization, first proposed by Chevallier and Polarski and later reintroduced by Linder has the following form:

$$w(a) = w_0 + w_a(1 - a) = w_0 + w_a \frac{z}{1 + z}, \quad (2.1)$$

where w_0 and w_a are the two parameters in the model. They represent the equation of state at present ($a = 1$) and its variation with respect to scale factor (or redshift). From the infinite past till the present time, the equation of state is bounded between $w_0 + w_a$ and w_0 . The dark energy density, in this case, evolves as:

$$\rho_{\text{DE}} \propto a^{-3(1+w_0+w_a)} e^{-3w_a(1-a)}. \quad (2.2)$$

This equation of state remarkably fits a wide range of scalar field dark energy models including the supergravity-inspired SUGRA dark energy models. The CPL parametrization is most commonly used in the literature to study the nature of dark energy. An outcome of the specific form of this parametrization is that, for $w_0 \geq -1$ and $w_a > 0$, the dark energy remains non-phantom in nature throughout the cosmological evolution; otherwise it shows phantom behavior at some point in time.

2.2 SS Parametrization

This parametrization was proposed by Scherrer and Sen [15] for slow-roll ‘thawing’ class of scalar field models having a canonical kinetic energy term. Later, it was shown [17] that this parametrization also holds true for the tachyon-type scalar field models having DBI-type kinetic energy term [18] as well as for phantom models for scalar fields having negative kinetic energy term. The main motivation for this parametrization was to look for a unique dark energy evolution for scalar field models that are constrained to evolve very close to the Cosmological Constant ($w = -1$). Since similar situations also arise in inflationary scenarios in the early universe, one assumes the same slow-roll conditions on the scalar field potentials as used in inflation. However, unlike the inflationary epoch, the situation differs due to the presence of the large matter content in the late universe; still it can be shown that under the assumption of the (i) two slow-roll conditions and that (ii) the scalar field is initially frozen at $w = -1$ due to large Hubble damping (termed ‘thawing class’), one gets a unique form for the dark energy equation of state irrespective of its potential. The form of this equation of state, for a universe with flat spatial hypersurface, is given by:

$$w(a) = (1 + w_0) \left[\sqrt{1 + (\Omega_{\text{DE}}^{-1} - 1)a^{-3}} - (\Omega_{\text{DE}}^{-1} - 1)a^{-3} \tanh^{-1} \frac{1}{\sqrt{1 + (\Omega_{\text{DE}}^{-1} - 1)a^{-3}}} \right]^2 \times \\ \times \left[\frac{1}{\sqrt{\Omega_{\text{DE}}}} - \left(\frac{1}{\Omega_{\text{DE}}} - 1 \right) \tanh^{-1} \sqrt{\Omega_{\text{DE}}} \right]^{-2} - 1. \quad (2.3)$$

This parametrization has one model parameter, w_0 , which represents its value at the present epoch together with the general cosmological parameter Ω_{DE} representing the present day dark energy density, which in a flat universe is related to the present day matter energy density through $\Omega_{\text{m}} + \Omega_{\text{DE}} = 1$. The energy density of this model of dark energy can be calculated analytically using the Friedmann equations which has been used in our analysis. At this point, it is worth pointing out that the recently constructed axionic quintessence model in string theory [28] can be described by this parametrization for certain range of parameters.

2.3 GCG Parametrization

The Chaplygin gas (CG) equation of state was first discussed in the cosmological context by Kamenshchik *et. al.* [29] and is described by

$$p = -\frac{c}{\rho}, \quad (2.4)$$

where c is an arbitrary constant and p and ρ represents the pressure and energy density of the CG fluid. Subsequently, this equation of state was generalized by Bento et al [11] and Bilic et al [30] as

$$p = -\frac{c}{\rho^\alpha}, \quad (2.5)$$

where α is a constant within the range $0 \leq \alpha \leq 1$. This form is known as the Generalized Chaplygin Gas (GCG) equation of state. In a later work Scherrer and Sen [12] considered the parameter range $\alpha < 0$ to describe diverse cosmological behaviors. Assuming a spatially homogeneous and isotropic universe along with the energy momentum conservation equation gives us

$$w(a) = -\frac{A}{A + (1 - A)a^{-3(1+\alpha)}}, \quad (2.6)$$

where $A = c/\rho_{\text{GCG}}^{1+\alpha}$. The GCG parametrization also contains two model parameters e.g A and α , similar to the CPL parametrization.

It is easy to check that the present equation of state is $w(0) = -A$. For $(1 + \alpha) > 0$, $w(a)$ behaves like a dust in the past and evolves towards negative values and becomes $w = -1$ in the asymptotic future. This is similar to ‘tracker/freezer’ behavior for a scalar field where it tracks the background matter in the past, and in the late time behaves like a dark energy with a negative equation of state. For $(1 + \alpha) < 0$, the opposite happens. In this case the $w(a)$ is frozen to $w = -1$ in the past and the slowly evolves towards higher values and eventually behaves like a dust in the future. This behavior is similar to the ‘thawing’ class of scalar field models. Moreover, in this case, the late time acceleration is a transient phenomena as the acceleration slows down eventually and the Universe enters again a dust regime. For both ‘thawing’ or ‘freezer’ kind of behaviors, the transition to/from $w = -1$ depends on the value of α . We shall consider both $1 + \alpha > 0$ and $1 + \alpha < 0$ to consider freezing as well as thawing type behaviors. However, we restrict $0 < A < 1$ only since for $A > 1$ singularity appears at

finite past. As a consequence, this model is restricted to probe dark energy behavior for non-phantom cases only, a feature which is also true for scalar field models with positive kinetic energy. This is akin to a strong theoretical prior on the model.

To summarize, we are considering three parametrization for the dark energy equation of state. The CPL parametrization has a simple linear dependence on scale factor which is true for dark energy behavior in general around present day but may not represent models that have more complicated scale factor dependence at slightly higher redshifts. The SS parametrization represents all slow-roll thawing class of scalar field models even if they are phantom in nature (i.e., having negative kinetic energies). The parametrization is also applicable for scalar fields with canonical kinetic energies as well as non-canonical kinetic energies. Hence, if dark energy is not Cosmological Constant but has small deviation from the Cosmological Constant, the SS is a good parametrization to consider. Moreover, the deviation from Cosmological Constant can be represented by a single parameter. Our third parametrization is the GCG parametrization which can describe both thawing as well as the freezer type behaviors of the scalar field models. It, however, restricts us to consider only non-phantom models. This parametrization can represent dark energy behaviors where the acceleration of the Universe have slowed down recently.

Finally, let us emphasize that while the CPL parametrization was proposed as a phenomenological form for the equation of state of dark energy, both the SS and GCG parametrizations were obtained from a specific field theory Lagrangian under certain conditions [11, 16].

3 Methodology

In this paper we have put constraints on the late time evolution history of dark energy by contrasting multiple dark energy models with CMB and low redshift observations. For CMB we have used the recent Planck C_ℓ^{TT} data. As Planck has not yet released the observed Polarization data, we have used WMAP-9 [31] low- ℓ polarization data for completeness, as has also been used in Planck analysis. In different frequency channels Planck has detected the CMB sky in much smaller scales ($\ell = 2500$) compared to WMAP. Planck has published two likelihood estimators [32], namely, the low- ℓ (2-49) likelihood which is estimated by **commander** and the high- ℓ (50-2500) which is estimated by **CAMBspec**, for four different frequency channels. At small scales, the foreground effects are dominant and there are 14 nuisance parameters [32, 33] corresponding to the foreground effects in different frequency channels. For our analysis with CMB data, we have always marginalized over these nuisance parameters. The cosmological model is described by the six cosmological parameters: $\Omega_b h^2$, $\Omega_{\text{CDM}} h^2$, θ , τ , A_s and n_s . First four parameters describe the background where Ω_b and Ω_{CDM} represent the baryon and the cold dark matter density and h represents the Hubble parameter. θ is the ratio of the sound horizon to the angular diameter distance at decoupling and τ is the reionization optical depth. A_s and n_s describes the amplitude and the spectral index of the primordial perturbation which we assume to be of the power-law form.

Finally, the CPL and GCG model have 2 parameters and SS model have one parameter describing the dark energy equation of state.

For non-CMB data, we have used Supernovae data, Baryon Acoustic Oscillations (BAO) data and data from Hubble space telescope. For Supernovae data we have used the recent Union 2.1 compilation [38] with 580 supernovae within redshifts $\sim 0.015 - 1.4$. We have used the covariance matrix of Union 2.1 compilation which includes systematic errors. For the Baryon Acoustic Oscillations we have used four datasets, namely the six-degree field galaxy survey [37], SDSS DR7 [34] and BOSS DR9 measurements [36] and the data from WiggleZ survey [35]. We confront the theoretical model with the distance ratio ($d_z = r_s(z_{\text{drag}})/D_V(z)$) measured by the particular surveys (and with the functions of d_z), where z_{drag} is the particular redshift where the baryon-drag optical depth becomes unity and $r_s(z_{\text{drag}})$ is the comoving sound horizon at that redshift. $D_V(z)$ is related to the angular diameter distance and the Hubble parameter at redshift z . For BAO we get constraints from 6 data points, of which three come from WiggleZ survey at 3 different redshifts ($z = 0.44, 0.6, 0.73$) and the other three come from the two SDSS measurements such as SDSS DR7 : $z = 0.35$, SDSS DR9 : $z = 0.57$ and a 6DF : $z = 0.106$). We have also used the HST data [39] which uses the nearby type Ia Supernova data with Cepheid calibrations to constrain the value of H_0 .

We have used the publicly available cosmological Boltzmann code CAMB [40, 41] to calculate the power spectrum for CMB and different observables for non-CMB observations and for the Markov Chain Monte Carlo analysis we have used the CosmoMC [42, 43]. In all the cases, we have taken into account the effect of dark energy perturbations though CAMB. Throughout our analysis we have fixed the number of relativistic species to be $N_{\text{eff}} = 3.046$.

4 Results

We start this section by showing, in Table 1, the best-fit χ_{eff}^2 values for cosmological models with different dark energy parametrizations. In obtaining the best-fits, we have used Powell’s BOBYQA method of iterative minimization [44] and the χ_{eff}^2 quoted are obtained from the joint analysis with CMB and all non-CMB data described in the previous section. We have also shown the breakdown of the χ_{eff}^2 from various datasets to clarify the preference of any individual dataset towards different dark energy models. Notice that the GCG parametrization, which is a non-phantom model, has similar χ_{eff}^2 values as in Λ CDM although it contains two extra parameters. This shows that if we restrict ourselves to non-phantom models - *a strong theoretical prior* - it is hard to distinguish them from a Λ CDM behavior as the best-fit value is always close to a model with $w = -1$. Allowing phantom behavior (i.e., for both CPL and SS parametrizations) results in marginally better fit to the complete datasets by a $\Delta\chi_{\text{eff}}^2 \sim \mathcal{O}(2 - 4)$. The improvement from Λ CDM for CPL model is 3.6 and for SS model is 2.6. This improvement in χ_{eff}^2 is, arguably, not large enough to justify the necessity to venture into the phantom regime.

Data	Λ CDM	CPL	GCG	SS
Planck (low- ℓ + high- ℓ)	7789.0	7787.4	7789.0	7788.1
WMAP-9 low- ℓ polarization	2014.4	2014.436	2014.383	2014.455
BAO : SDSS DR7	0.410	0.073	0.451	0.265
BAO : SDSS DR9	0.826	0.793	0.777	0.677
BAO : 6DF	0.058	0.382	0.052	0.210
BAO : WiggleZ	0.020	0.069	0.019	0.033
SN : Union 2.1	545.127	546.1	545.131	545.675
HST	5.090	2.088	5.189	2.997
Total	10355.0	10351.4	10355.0	10352.4

Table 1. Best fit χ^2_{eff} obtained for different models upon comparing against CMB + non-CMB datasets. The breakdown of the χ^2_{eff} for individual data are also provided. To obtain the best-fit we have used the Powell’s BOBYQA method of iterative minimization.

It is clear from Table 1, where the total and the individual χ^2_{eff} are given, that the Supernova data marginally favors the concordance Λ CDM model as well as the non-phantom GCG model compared to other two parametrizations. Planck data prefers lower H_0 for Λ CDM which does not agree well with the H_0 from HST and the fit to HST gets worse. However CPL and SS models allowing phantom equation of state fit the data from both CMB and HST better than cosmological constant at their best fit values. A direct upshot of these phantom equation of state that fits the CMB data better than the Λ CDM model is that it comes with higher value of H_0 that in turn agrees with the HST data better too. However, for the same choice of best fit parameter values they do not provide similar improvement in χ^2_{eff} for Supernovae data. This indicates that SN data favors the equation of states closer to the cosmological constant. The breakdown of χ^2_{eff} points to the tantalizing possibility that different datasets, which effectively probe different epochs in the history of our Universe, prefer different kind of dark energy behaviors. The improvement in the total χ^2_{eff} for the CPL and SS model over Λ CDM and GCG is driven by the ability to have a higher H_0 albeit along with the associated preference for phantom behavior. However, to be conclusive, one would need to evaluate the full likelihood behavior for the different models w.r.t the diverse datasets.

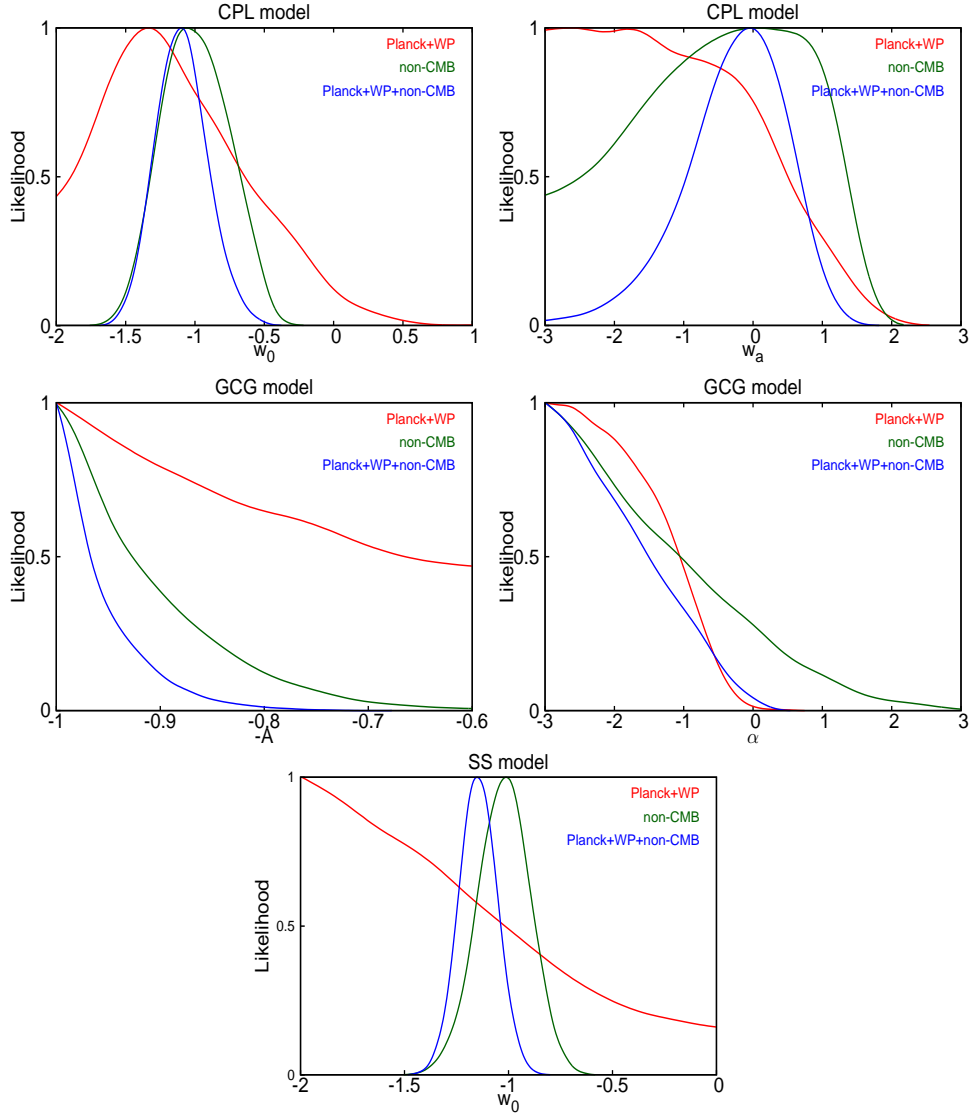


Figure 1. The likelihood functions for different parameters of equation of state. The upper ones are for the CPL parametrization, the middle ones for the GCG parametrization and the bottom one is for the SS parametrization. The color codes are for different analysis with different observational data and are described in the plot.

In Table 2, we quote the mean values as well as the 1σ errors bars for different parameters ($\Omega_b h^2$, $\Omega_{\text{CDM}} h^2$, θ , τ , n_s , A_s , w_0 , w_a and the derived matter content Ω_m and Hubble constant H_0). For each parameter, the first row contains results from CMB datasets, the second row contains the results when we combine high and low redshift data and the last row provides the results from non-CMB datasets. Note that bounds on H_0 becomes considerably weak for CMB analysis alone when we allow phantom equation of state through CPL and SS. In all the cases w_0 ($-A$ for GCG) is better constrained with non-CMB data compared to the CMB data alone since w_0

	CPL	SS	GCG
$\Omega_b h^2$	0.0221 ± 0.00028 0.022 ± 0.00026 $0.027^{+0.004}_{-0.005}$	0.0221 ± 0.00026 $0.0221^{+0.00026}_{-0.00024}$ $0.028^{+0.004}_{-0.006}$	0.022 ± 0.00028 0.0223 ± 0.00024 0.029 ± 0.005
$\Omega_{\text{CDM}} h^2$	0.1196 ± 0.0027 0.1209 ± 0.0023 $0.126^{+0.014}_{-0.017}$	0.1198 ± 0.0026 0.1192 ± 0.0018 $0.128^{+0.014}_{-0.018}$	$0.1199^{+0.0026}_{-0.0028}$ 0.117 ± 0.0015 $0.127^{+0.015}_{-0.018}$
100θ	1.041 ± 0.0006 1.041 ± 0.0006 1.042 ± 0.023	1.041 ± 0.0006 1.041 ± 0.00056 1.048 ± 0.022	1.041 ± 0.0006 1.042 ± 0.00056 $1.05^{+0.019}_{-0.027}$
τ	$0.09^{+0.012}_{-0.014}$ $0.087^{+0.012}_{-0.014}$ -	$0.09^{+0.012}_{-0.015}$ 0.091 ± 0.013 -	$0.09^{+0.013}_{-0.014}$ 0.094 ± 0.014 -
$w_0[-A]$	$-1.13^{+0.37}_{-0.66}$ $-1.005^{+0.15}_{-0.17}$ $-0.995^{+0.23}_{-0.27}$	$-1.31^{+0.19}_{\text{unbounded}}$ $-1.14^{+0.08}_{-0.09}$ -1.02 ± 0.12	$-0.827^{+0.06}_{\text{Non-phantom prior cut}}$ $-0.957^{+0.007}_{\text{Non-phantom prior cut}}$ $-0.92^{+0.018}_{\text{Non-phantom prior cut}}$
$w_a[\alpha]$	$-1.15^{+0.6}_{\text{unbounded}}$ $-0.48^{+0.77}_{-0.54}$ $-0.5^{+1.64}_{-0.94}$	- - -	$-1.97^{+0.32}_{\text{unbounded}}$ $-2.0^{+0.29}_{\text{unbounded}}$ $-1.49^{+0.4}_{\text{unbounded}}$
n_s	0.9607 ± 0.007 $0.9579^{+0.0063}_{-0.0066}$ -	0.9603 ± 0.007 $0.9619^{+0.0059}_{-0.0057}$ -	$0.9603 \pm +0.00073$ $0.9669^{+0.00056}_{-0.00059}$ -
$\ln[10^{10} A_s]$	$3.089^{+0.023}_{-0.027}$ $3.087^{+0.024}_{-0.026}$ -	$3.089^{+0.023}_{-0.028}$ 3.091 ± 0.025 -	3.09 ± 0.025 3.092 ± 0.026 -
Ω_m	$0.239^{+0.028}_{-0.099}$ $0.291^{+0.011}_{-0.013}$ 0.29 ± 0.024	$0.27^{+0.04}_{-0.1}$ $0.288^{+0.012}_{-0.013}$ $0.298^{+0.02}_{-0.026}$	$0.344^{+0.022}_{-0.032}$ $0.304^{+0.009}_{-0.011}$ $0.3^{+0.021}_{-0.024}$
H_0	$80^{+17.8}_{-7.8}$ 70.26 ± 1.4 72.68 ± 2.2	$74.8^{+13.3}_{-9.8}$ 70.3 ± 1.4 72.67 ± 2.15	$64.6^{+2.61}_{-1.91}$ $67.9^{+0.9}_{-0.7}$ 72.4 ± 2.16

Table 2. The mean values and the 1σ ranges for different cosmological parameters from our analysis. CPL, SS and GCG marks the dark energy parametrization used. The parameters w_0 and w_a represents $-A$ and α for GCG model and have been indicated in the table. For each parameters the first, second and last row indicate the results from the analysis with CMB, CMB + non-CMB and non-CMB datasets respectively.

determines the behavior of dark energy model at low redshift. However, w_a (α for

GCG) is constrained better by CMB datasets for CPL and GCG as it determines the change in the dark energy equation of state throughout the expansion of Universe. It is clear that CPL and SS allow lower Ω_m and higher H_0 whereas the GCG allows higher Ω_m and lower H_0 consistently for all the analyses ¹. It should be noted that for CPL model the mean value of H_0 for the analysis with CMB datasets comes out to be 80 and the 1σ uncertainty stretches the upper bound to 98. For SS model the bound on H_0 CMB *only* analysis is better than CPL since the model has one dark energy parameter and therefore less degenerate.

Having described the best-fit χ^2_{eff} and the allowed ranges for different parameters, we now discuss the likelihoods of parameters for the different dark energy parametrization. These likelihoods are shown in Figure 1. Interestingly, in CPL as well SS parametrization, the CMB data from Planck takes the present value of equation of state (w_0) towards higher phantom values ² whereas the non-CMB data brings it closer to the Cosmological Constant ($w_0 = -1$). For the combined datasets, we find that the mean w_0 comes close to the Cosmological Constant ($w = -1$) but still stays in the phantom region.

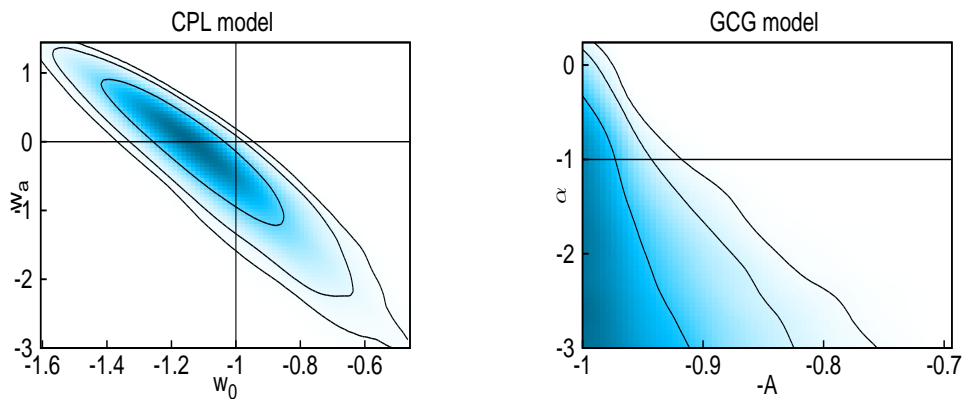


Figure 2. Contour plots in the $w_0 - w_a$ plane for CPL and $A - \alpha$ plane for the GCG parametrization.

One can argue that there remains a tension between CMB and non-CMB data which questions the effectiveness of a joint analysis of CMB plus non-CMB data together in future. However, it is hard to pull out a decisive argument from these plots whether and to what extent the Cosmological Constant is consistent with the data. For a better understanding, we need to look at the 2D marginalized contours of dark energy equation of state parameters.

¹For analysis with non-CMB datasets GCG indicates a higher value of H_0

²Basically w_0 it is unconstrained in the phantom direction (with CMB only) upto the prior range considered.

In Figure 2, we show the marginalized 2D contour plots in $w_0 - w_a$ and $A - \alpha$ parameter plane for CPL and GCG parametrization respectively. The CPL case confirms the results earlier obtained by the Planck collaborations³. It shows that the Cosmological Constant behavior ($w_0 = -1, w_a = 0$) is disallowed at 1σ confidence level. Moreover the region $w_0 > -1$ and $w_a > 0$ is highly constrained even at 3σ confidence level showing that it is very unlikely that dark energy behaved in non-phantom manner at all epochs.

For GCG parametrization (which is valid only for non-phantom region), as seen in Figure 2, from the relative shaded region below and above the $\alpha = -1$ horizontal line we find that the thawing behavior ($\alpha < -1$) is more probable than the freezing behavior ($\alpha > -1$) for dark energy. We would like to highlight that CMB and non-CMB data, in this context of GCG models, qualitatively distinguishes the equation of state of dark energy. For example, while the CMB data constrains the value of α from above, non-CMB can not provide a bound there. On the other hand, in constraining $-A$, the opposite happens. Since, non-CMB data (mainly SN) provides the most stringent constraints at the present epoch it can constrain A much better than CMB data from Planck. However SN data does not provide any information beyond $z \sim 1.4$ and therefore can not constrain α as good as CMB data. Note that for $1 + \alpha > 0$ the denominator of Eq. 2.6) diverges at high redshift (small a) and makes $w \simeq 0$ (regardless of A) which is not supported by CMB data. This result clearly shows the sensitivity of two different probes toward two different parameters in the dark energy equation of state. Here, unlike the CPL and SS parametrizations, we can argue that CMB and non-CMB data may go through a joint analysis in order to obtain a tighter constraint on the dark energy equation of state. For both CPL and SS parametrization (that allow phantom behavior), phantom type equation of state is preferred for CMB+non-CMB data. Hence, irrespective of the equation of state parametrization with different number of parameters, phantom is preferred behavior for combined data. We should point out that allowing the phantom region in the parameter space brings in tension between CMB and non-CMB (specifically SN data); note that there is no tension between them when we just concentrate on the non-phantom scenarios. At this point we would like to stress on the issue that if the two data sets do not have any systematic effects and we claim that a reasonable theory should explain the cosmology obtained from different observational data to similar extent, our results highlights the interesting possibility of exploring and expanding theoretical ideas of dark energy which can fundamentally supports an equation of state which evolves from a phantom nature at high redshifts towards a Cosmological Constant behavior at low redshifts may resolve the tension.

Next, we look at 2D confidence regions for other cosmological parameters. In Figure 3, we show the confidence contours in the $w_0 - H_0$ plane for all three dark energy parametrizations. The Planck best-fit measurements for H_0 for a concordance Λ CDM model is shown by the horizontal red line. The vertical black line represents Cosmological Constant. In Figure 4, we show the confidence contours in the $\Omega_m - H_0$ parameter plane for all three parametrization; the red lines show the best-fit values for

³A tiny deviation from the Planck result is mainly due to use of all the non-CMB data together in our analysis

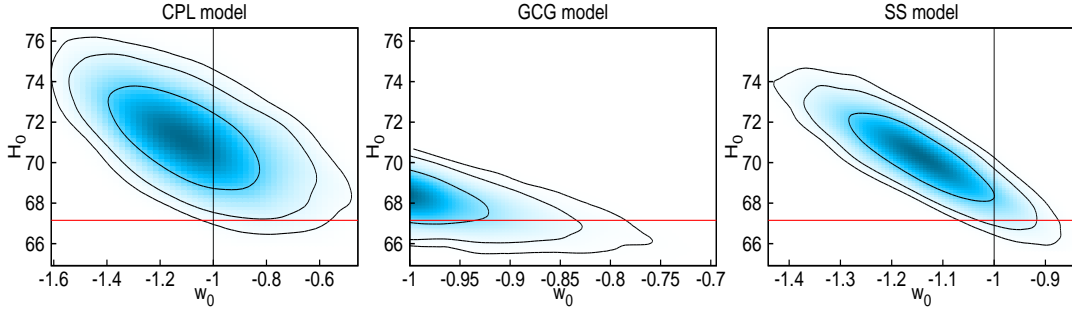


Figure 3. Contour plots in $w_0 - H_0$ parameter plane for CPL (left), GCG (middle) and SS (right) parametrization. The red line represents the best-fit value for H_0 obtained from Planck for Λ CDM case.

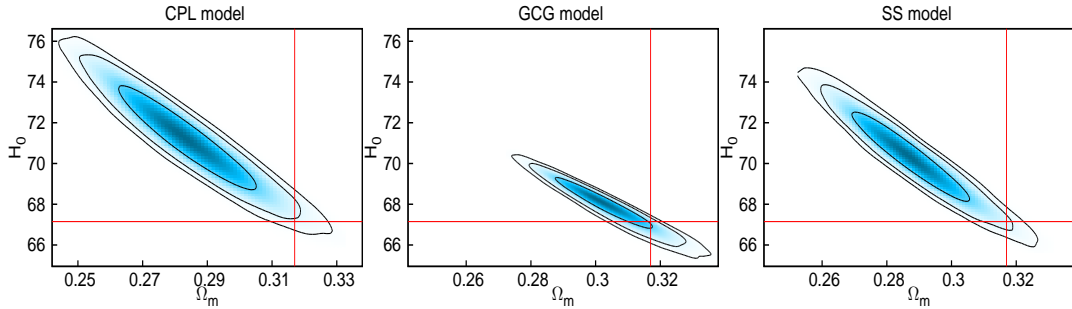


Figure 4. Contour plots in $\Omega_m - H_0$ parameter plane for CPL (left), GCG (middle) and SS (right) parametrization. The red lines represent the best-fit values for H_0 and Ω_m obtained from Planck for Λ CDM model.

Ω_m and H_0 as measured by Planck for a concordance Λ CDM model. At this stage, let us mention that overplotting the Planck best-fit values does not imply any consistency or inconsistency of different datasets. Our aim is to address the issue of phantom behavior of the dark energy, i.e. whether it is allowed and, if allowed, to what extent does that affect the constraints on other cosmological parameters?

A look at Figures 3 and 4 show that if we allow phantom equation of state (*i.e.* for CPL and SS parametrizations), the best fit cosmology shifts to a higher value of H_0 and lower value of Ω_m . This shift leaves the base Λ CDM values measured by Planck outside 2σ confidence limit for dark energy models captured by the CPL parametrization and at the border of 2σ contour in case of SS parametrized models. However, for dark energy models described by the GCG parametrization - which does not allow phantom models - the Planck Λ CDM values are at the border of the 1σ C.L.. To summarize, Planck measurements of high Ω_m and low H_0 values for Λ CDM model are consistent

with measurements of these two parameters using both CMB + non-CMB data *if* we restrict ourselves only to non-phantom models like GCG. However, tension arises when we allow phantom behavior, as the CMB and non-CMB data drag the equation of state in two different directions (i.e., both phantom and non-phantom) and the phantom region provides better fit to the joint likelihood of CMB and non-CMB by dominantly better fitting Planck data (in the joint analysis).⁴

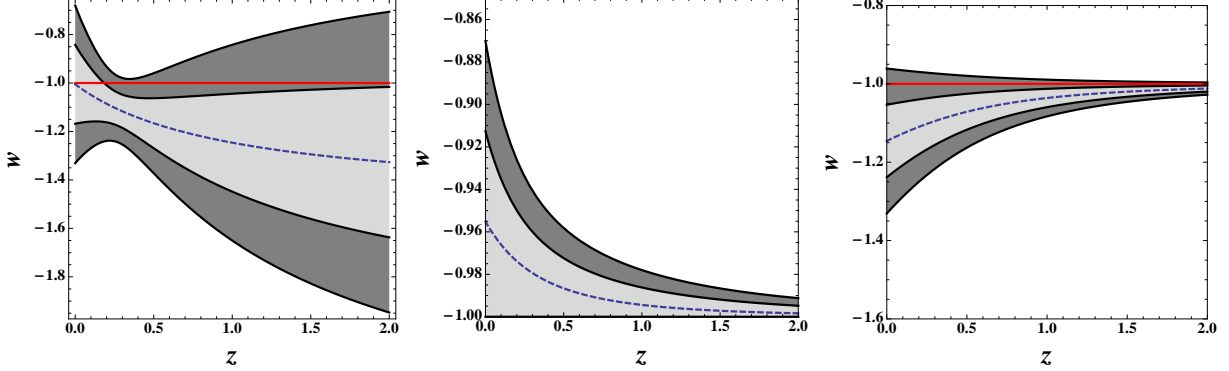


Figure 5. Behavior of equation of state w as a function of redshift z for CPL (left), GCG (middle) and SS (right) parametrization for $1 - \sigma$ and $2 - \sigma$ confidence level. The red and blue lines correspond to $w = -1$ and the mean w respectively.

The behaviors of the equation of state as a function of redshift at 1σ and 2σ confidence levels, for the three parametrizations, are shown in Figure 5.

A) It is apparent that SS parametrization (right panel in the figure) constrains the equation of state to evolve very closely to the $w = -1$; the 1σ region for w is always less than but within $\sim 5\%$ to the Cosmological Constant at all epochs. This is expected as this parametrization represents thawing class scalar field models with small deviations from Cosmological Constant. Thus, the non-phantom behavior is not allowed at 1σ confidence level. However, at 2σ , the dark energy behavior is consistent with a Cosmological Constant. Note, that the mean w is always phantom and can provide reasonable deviation from Cosmological Constant behavior at the present epoch.

B) The CPL parametrization (left panel in the figure) has similar behavior and dark energy appears to be phantom at more than 1σ level beyond $z > 0.2$. Only at $z < 0.2$, we get $w = -1$ line within the 1σ bound. For $z < 0.2$, the mean equation of state touch $w = -1$ from below. In this parametrization, mean dark energy equation of state starts as a Cosmological Constant at only $z = 0$ and quickly deviates from it to become phantom like as redshift increases. w is best constrained at roughly around $z \sim 0.3$. Note that dark energy with $w \geq -1$ lies outside the inner grey region (1σ) in the range ($0.2 < z < 2$). Moreover, it needs the equation of state parameters to be

⁴Note, again, that due to the phantom behavior, a higher value of H_0 is favored involving Planck data which is in better agreement with HST.

extremely fine tuned to have $w \geq -1$ around $z \simeq 0.3$ and still be inside the 2σ band. Contrary to the SS parametrization, the CPL parametrization poorly constrain w at higher z , whereas at the present epoch both constrain w at roughly 20 – 30% level. This behavior of the equation of state is consistent with what we observe in the $w_0 - w_a$ confidence plane as discussed earlier. To summarize, w is consistent with Λ CDM only at $z = 0$ but is increasingly phantom like with increasing redshift ⁵.

It is easy to understand the different behavior w for SS and CPL parametrizations. SS parametrization is designed to follow $w = -1$ in early epoch and has flexibilities only at low redshifts. CPL, on the other hand, can allow more scenarios with one more degree of freedom. The important similarity between them is both the solution permit larger area in phantom region. Note that the SS mean w is allowed within the CPL 1σ bounds. The tighter Constraints on w for SS model at high redshift is also reflects the inability of SS model to depart from $w = -1$ at early epochs.

C) The mean equation of state for the GCG parametrization (middle panel in the figure) shows that w reaches the value ≈ -0.96 at present epoch, having started close to or at $w = -1$ at high redshifts. The error bars clearly point towards thawer class of models and hence provides an important constraint for scalar field models for dark energy. For this class of models, in the entire redshift range, the deviation of the mean w from a Cosmological Constant is far less than what are found for the other classes of models.

To summarize, one of our central results is that if one allows for phantom behavior in the dark energy equation of state, the phantom region provides a better fit to the combined CMB and non-CMB data. Provided that CMB and non-CMB joint analysis does not impose systematic errors as has been discussed before, *our results can therefore be thought of as an invitation to construct models of dark energy which lead to phantom behavior*, at least at the scales probed by the Planck and non-CMB observations.

5 Conclusions

The post-Planck era has seen cosmological parameters best constrained till date using a CMB and a host of non-CMB measurements. This raises the possibility of precision determination of the nature of dark energy. In this paper we do a detail investigation with such an aim in mind ⁶. Currently, almost all the cosmological constraints on dark energy is based on a single parametrization, e.g. the CPL parametrization. However, theoretical models of dark energy abound in the literature, which leads to possibilities of having models that may not be fairly represented by such a parametrization. Question remain as to whether there are possible dark energy evolutions that one misses using the CPL parametrization.

⁵Similar conclusions about the phantom behavior of dark energy has recently reported by the Pan-STARRS1 survey [46].

⁶After we submitted our paper to the arXiv, a similar study and very similar conclusions were shown in [47]

To address the above mentioned question we work with two other parametrizations, namely SS and GCG, apart from CPL. The SS model, which describes the dynamical equation of state with a single parameter, allows both phantom and non-phantom behavior and probes deviations close to the Cosmological Constant. The GCG model, on the other hand, represents only non-phantom models allowing *only* positive kinetic energies of underlying scalar field model and provides a clear distinction between tracker and thawer models. Finally, while the CPL parametrization was proposed as a phenomenological form for the equation of state of dark energy, both the SS and GCG parametrizations were obtained from a specific field theory Lagrangian under certain conditions [11, 16]. Hence, the three parametrizations together probe maximally possible parameter space for dark energy models.

Having the three parametrizations in hand, we use CMB and non-CMB data in a separate and combined analysis to look at dark energy behaviors. The main results of this study are summarized below:

- We find that *if* we allow phantom behavior of dark energy, irrespective of misgivings to its use due to the negative kinetic energy of scalar fields, then CMB data favors phantom over non-phantom behavior with high confidence. On the other hand non-CMB data prefer non-phantom behavior for every parametrization considered. Once phantom behavior is allowed (*i.e.* in CPL & SS parametrizations), the combined CMB + non-CMB data allows regions such that the Cosmological Constant ($w = -1$) is pushed outside than 1σ confidence level contour. Any tension between CMB and non-CMB datasets may be attributed to unknown systematics or the lack of a better theory/parametrization of the dark energy equation of state.
- Using the correlation between the equation of state parameters, we reconstruct the late time (*i.e.* $z < 2$) evolution of dark energy. For the SS models, the $w = -1$ line stays outside 1σ reconstructed band of the evolution history of dark energy for the entire redshift range. In the case of CPL model, the $w = -1$ line stays outside 1σ region for $z > 0.2$.
- The GCG parametrization, which are theoretically constructed so as not to allow phantom models, shows consistency between CMB and non-CMB data although they have worse likelihood than other parametrizations. It is found that the CMB and non-CMB observations are separately sensitive to the two parameters of the GCG parametrization and that the joint constraint is consistent with the Cosmological Constant. For these models, the cosmological parameters too are consistent with base Planck best-fit measurements. Allowing phantom behavior of dark energy reveals tension between CMB and non-CMB (mainly SNe) data since CMB data (from Planck) prefers the phantom dark energy behavior and on the other hand non-CMB data prefers cosmological constant and non phantom behavior.
- From the results obtained with the three parametrizations, it comes out that for scalar field dark energy models, a thawing behavior is more probable than the

freezing behavior. This is most clearly been demonstrated in GCG models. Such an outcome is particularly interesting in the context of recent construction of axionic quintessence model in string theory [28] which is of thawing nature [45].

- The constraints on dark energy, coming out of a joint analysis of all available data, differ from model to model. Not only does the mean w depends on the parametrization of choice but also the error bar on the mean has different behavior. For SS and GCG parametrization, the nature of dark energy is best constrained at high redshifts; however, for the CPL parametrization the best constraints come in the redshift range of $\approx 0.2 - -0.3$.
- It has been already noticed in the cosmology community that the Planck measurement for the parameters Ω_m and H_0 for the Λ CDM model is in tension with the similar measurements by the HST. We find that for SS and CPL parametrizations, where we allow phantom, a better fit to the data comes with a large value of H_0 which helps to agree better with the HST data. In fact, the improvement in the total χ^2_{eff} for the CPL and SS model over Λ CDM and GCG is driven by the ability to have a higher H_0 albeit along with the associated preference for phantom behavior. However, in these parametrizations, the phantom effect drags the background cosmological parameter space in such a way that the corresponding best-fit base model and that from Planck becomes 2σ away from each other. This implies that if we include phantom model in our theoretical framework in any cosmological calculations, then we are not allowed to work with Planck values for the base Λ CDM background parameters. However, GCG model, the only pure non-phantom model, shows that, within the allowed range of dark energy equation of state, the background cosmological parameters are in agreement with Planck values for Λ CDM.

Also, note that when we allow phantom behavior, the H_0 becomes highly degenerate with dark energy equation of state in case of CMB only measurements. Other parametrizations which allow non phantom behaviors only does not exhibit similar behavior; the H_0 errors for CPL is ≈ 5 times larger compared to GCG for CMB only, even though both have the same number of degrees of freedom.

The conclusions drawn above, in the current work, comes from a joint analysis of CMB and non-CMB data using different evolving dark energy models having different parametrization of the equation of state of dark energy. In a detailed analysis of SNe data (along with other datasets), the PAN-STARRS1 survey [46] recently found hints for similar phantom behavior of dark energy, although using a constant equation of state. Their value of w is inconsistent with the Cosmological Constant value of -1 at $> 2\sigma$ level (if used along with Planck data) or at $< 2\sigma$ (if used along with WMAP9 data). Recently, in an arXiv submission [47] following our work, it was also reported that for dataset Planck+HST+BAO+SNLS3 the Λ CDM model is just outside the 2σ confidence regime, while for the dataset WMAP9+HST+BAO+SNLS3 the Λ CDM model is 1σ away from the best fit. All these works nicely complements each other.

A very important point, not adequately appreciated in the literature (and missed in the two papers [46, 47] cited above), comes out in Figure 5. This is the fact that *our constraints on w and hence the nature of dark energy that we infer from cosmological observation depends crucially on the choice of the underlying parametrization of the equation of state*. In fact, (any) deviation of w from a Cosmological Constant, with redshift depends on the parametrization - whereas for the current available data, both SS and GCG infer dark energy being close to the Cosmological Constant at high redshift but ‘deviating from it in two different directions’ when we approach current epoch; on the other hand CPL is close to Cosmological Constant at current epoch and deviates away at high z . Given this trichotomy, it is important to do non-parametric reconstruction of w for the total dataset to infer the correct nature of dark energy without any prior on form of w .

To summarize once again, we have done the most comprehensive study of dark energy equation of state constraints from a joint analysis of Planck CMB data along with SNe, BAO and H_0 data. A central results of our analysis is that if one allows for phantom behavior in the dark energy equation of state, the phantom region provides a better fit to the combined CMB and non-CMB data. The tension with Λ CDM can be due to the even more mysterious nature of dark energy or a combination of chance and systematic errors. Our results motivate the construction of models of dark energy which lead to phantom behavior. This means going beyond standard possibilities for dark energy involving a scalar field with a positive kinetic energy term only which do not lead to a violation of the weak energy condition. However, it is well known that in consistent theories of gravity, like string theory, the weak energy condition and also the null energy condition can be violated due to the presence of higher derivative corrections [48]. We leave it as an intriguing question to the reader as to whether such violations can be used to construct a model of dark energy which would fit the data better than say a positive Cosmological Constant.

Acknowledgments

The authors would like to thank Sandip Trivedi for motivation, discussions and support throughout the project. D.K.H wish to acknowledge support from the Korea Ministry of Education, Science and Technology, Gyeongsangbuk-Do and Pohang City for Independent Junior Research Groups at the Asia Pacific Center for Theoretical Physics. We also acknowledge the use of publicly available CAMB and CosmoMC in our analysis. A.A.S. acknowledges the funding from SERC, Dept. of Science and Technology, Govt. of India through the research project SR/S2/HEP-43/2009. SP thanks ISI, Kolkata for support through research grant. This project is part of the Dark Universe Initiative program.

References

- [1] E. J. Copeland, M. Sami and S. Tsujikawa, Int. J. Mod. Phys. D **15**, 1753 (2006); Miao Li, Xiao-Dong Li, Shuang Wang, arXiv:1103.5870; V. Sahni and

- A. A. Starobinsky, *Int. J. Mod. Phys. D* **9**, 373 (2000); S. M. Carroll, *Living Rev. Rel.* **4**, 1 (2001); P. J. E. Peebles and B. Ratra, *Rev. Mod. Phys.* **75**, 559 (2003); T. Padmanabhan, *Phys. Rept.* **380**, 235 (2003).
- [2] A. G. Riess, et al., *Astron. J.* **116**, 1103, (1998); A. G. Riess, et al., *Astrophys. J.*, **607**, 665, (2004); S. Perlmutter, et al., *Astrophys. J.*, **517**, 565, (1999); J. L. Tonry, et al., *Astrophys. J.*, **594**, 1, (2003); R. A. Knop, et al., *Astrophys. J.*, **598**, 102, (2003); R. Amanullah, et al., *Astrophys. J.*, **716**, 712, (2010); N. Suzuki et al., *Astrophysics J.* **746**, 85 (2012).
- [3] E. Komatsu et al., *Astrophys. J. Suppl.* **192**, 18 (2011).
- [4] See,
http://www.sciops.esa.int/index.php?project=planck&page=Planck_Collaboration
- [5] D. Eisenstein, *Astrophys. J.*, **633**, 560 (2005).
- [6] S. Kachru, R. Kallosh, A. D. Linde, J. M. Maldacena, L. P. McAllister and S. P. Trivedi, *JCAP* **0310**, 013 (2003) [hep-th/0308055]
- [7] B. Ratra and P.J.E. Peebles, *Phys. Rev. D*, **37**, 3406 (1988); M.S. Turner and M. White, *Phys. Rev. D*, **56**, R4439 (1997) R.R. Caldwell, R. Dave, and P.J. Steinhardt, *Phys. Rev. Lett.* **80**, 1582 (1998); A.R. Liddle and R.J. Scherrer, *Phys. Rev. D*, **59**, 023509 (1999); P.J. Steinhardt, L. Wang, and I. Zlatev, *Phys. Rev. D*, **59**, 123504 (1999); R. J. Scherrer and A. A. Sen, *Phys. Rev. D*, **77**, 083515 (2008).
- [8] C. Armendariz-Picon, T. Damour, and V. Mukhanov, *Phys. Lett. B* **458**, 209 (1999); J. Garriga and V.F. Mukhanov, *Phys. Lett. B* **458**, 219 (1999); T. Chiba, T. Okabe, M. Yamaguchi, *Phys. Rev. D*, **62**, 023511 (2000); C. Armendariz-Picon, V. Mukhanov, and P.J. Steinhardt, *Phys. Rev. Lett.* **85**, 4438 (2000); C. Armendariz-Picon, V. Mukhanov, and P.J. Steinhardt, *Phys. Rev. D*, **63**, 103510 (2001); T. Chiba, *Phys. Rev. D*, **66**, 063514 (2002); L.P. Chimento and A. Feinstein, *Mod. Phys. Lett. A* **19**, 761 (2004); L.P. Chimento, *Phys. Rev. D*, **69**, 123517 (2004); R.J. Scherrer, *Phys. Rev. Lett.* **93**, 011301 (2004).
- [9] R. R. Caldwell, *Phys. Lett. B* **545**, 23 (2002).
- [10] J. S. Bagla, H. K. Jassal and T. Padmanabhan, *Phys. Rev. D* **67**, 063504 (2003); A. A. Sen, *JCAP*, **0603**, 010, (2006).
- [11] M.C. Bento, O. Bertolami, and A.A. Sen, *Phys. Rev. D*, **66**, 043507 (2002)
- [12] A. A. Sen and R. J. Scherrer, *Phys. Rev. D*, **72**, 063511 (2005).
- [13] M. Chevallier and D. Polarski, *Int. J. Mod. Phys. D* **10**, 213 (2001) [gr-qc/0009008].
- [14] E. V. Linder, *Phys. Rev. Lett.* **90**, 091301 (2003) [astro-ph/0208512].
- [15] R. J. Scherrer and A. A. Sen, *Phys. Rev. D* **77**, 083515 (2008) [arXiv:0712.3450 [astro-ph]].
- [16] R. J. Scherrer and A. A. Sen *Phys. Rev. D* **78**, 067303 (2008)
- [17] A. Ali, M. Sami and A. A. Sen, distinguish it from quintessence ?," *Phys. Rev. D* **79**, 123501 (2009) [arXiv:0904.1070 [astro-ph.CO]].
- [18] E. Bergshoeff, M. de Roo, T. de Wit, E. Eyras and S. Panda, *JHEP* **0005** 009(2000).

- [19] M. C. Bento, O. Bertolami and A. A. Sen, Gen. Rel. Grav. **35**, 2063 (2003) [gr-qc/0305086].
- [20] M. C. Bento, O. Bertolami and A. A. Sen, astro-ph/0210375.
- [21] M. C. Bento, O. Bertolami and A. A. Sen, Phys. Rev. D **67**, 063003 (2003) [astro-ph/0210468].
- [22] M. C. Bento, O. Bertolami and A. A. Sen, Phys. Lett. B **575**, 172 (2003) [astro-ph/0303538].
- [23] S. Thakur, A. Nautiyal, A. A. Sen and T. R. Seshadri, Mon. Not. Roy. Astron. Soc. **427** (2012) 988 [arXiv:1204.2617 [astro-ph.CO]].
- [24] A. Shafieloo, Mon. Not. Roy. Astron. Soc. **380**, 1573 (2007) [astro-ph/0703034 [ASTRO-PH]].
- [25] A. Shafieloo, JCAP **1208**, 002 (2012) [arXiv:1204.1109 [astro-ph.CO]].
- [26] A. Shafieloo, V. Sahni and A. A. Starobinsky, Phys. Rev. D **80**, 101301 (2009) [arXiv:0903.5141 [astro-ph.CO]].
- [27] Jun-Qing Xia, Hong Li and Xinmin Zhang, Phys. Rev. D **88**, 063501 (2013); Valeria Pettorino, arXiv:1305.7457 [astro-ph.CO]; Valentina Salvatelli and Andrea Marchini, Phys. Rev. D **88**, 023531 (2013); E. Macaulay, I. K. Wehus and H. K. Eriksen, arXiv:1303.6583 [astro-ph.CO]; C. Cheng and Q. -G. Huang, arXiv:1306.4091 [astro-ph.CO].
- [28] Sudhakar Panda, Yoske Sumimoto and Sandip P. Trivedi, Phys. Rev. D **83**, 083506 (2011).
- [29] A. Y. Kamenshchik, U. Moschella and V. Pasquier, Phys. Lett. B **511** (2001) 265 [gr-qc/0103004].
- [30] N. Bilic, G. B. Tupper, and R. D. Viollier, Phys. Lett. B **535**, 17 (2002);
- [31] G. Hinshaw *et al.* [WMAP Collaboration], arXiv:1212.5226 [astro-ph.CO].
- [32] P. A. R. Ade *et al.* [Planck Collaboration], arXiv:1303.5075 [astro-ph.CO].
- [33] P. A. R. Ade *et al.* [Planck Collaboration], arXiv:1303.5076 [astro-ph.CO].
- [34] W. J. Percival *et al.* [SDSS Collaboration], Mon. Not. Roy. Astron. Soc. **401**, 2148 (2010) [arXiv:0907.1660 [astro-ph.CO]].
- [35] C. Blake, E. Kazin, F. Beutler, T. Davis, D. Parkinson, S. Brough, M. Colless and C. Contreras *et al.*, Mon. Not. Roy. Astron. Soc. **418**, 1707 (2011) [arXiv:1108.2635 [astro-ph.CO]].
- [36] L. Anderson, E. Aubourg, S. Bailey, D. Bizyaev, M. Blanton, A. S. Bolton, J. Brinkmann and J. R. Brownstein *et al.*, Mon. Not. Roy. Astron. Soc. **427**, no. 4, 3435 (2013) [arXiv:1203.6594 [astro-ph.CO]].
- [37] F. Beutler, C. Blake, M. Colless, D. H. Jones, L. Staveley-Smith, L. Campbell, Q. Parker and W. Saunders *et al.*, Mon. Not. Roy. Astron. Soc. **416**, 3017 (2011) [arXiv:1106.3366 [astro-ph.CO]].
- [38] N. Suzuki, D. Rubin, C. Lidman, G. Aldering, R. Amanullah, K. Barbary, L. F. Barrientos and J. Botyanszki *et al.*, Astrophys. J. **746**, 85 (2012)

- [arXiv:1105.3470 [astro-ph.CO]].
- [39] A. G. Riess, L. Macri, S. Casertano, H. Lampeitl, H. C. Ferguson, A. V. Filippenko, S. W. Jha and W. Li *et al.*, *Astrophys. J.* **730**, 119 (2011) [Erratum-ibid. **732**, 129 (2011)] [arXiv:1103.2976 [astro-ph.CO]].
 - [40] A. Lewis, A. Challinor and A. Lasenby, *Astrophys. J.* **538** (2000) 473 [astro-ph/9911177].
 - [41] See, <http://camb.info/>.
 - [42] A. Lewis and S. Bridle, *Phys. Rev. D* **66** (2002) 103511 [astro-ph/0205436].
 - [43] See, <http://cosmologist.info/cosmomc/>.
 - [44] M. J. D. Powell, Cambridge NA Report NA2009/06, University of Cambridge, Cambridge (2009).
 - [45] G. Gupta, S. Panda and A. A. Sen, *Phys. Rev. D*, **85**, 023501 (2012) S. Kumar, S. Panda and A. A. Sen, *Class. Quant. Grav.* **30**, 155011 (2013).
 - [46] A. Rest, D. Scolnic, R. J. Foley, M. E. Huber, R. Chornock, G. Narayan, J. L. Tonry and E. Berger *et al.*, arXiv:1310.3828 [astro-ph.CO].
 - [47] B. Novosyadlyj, O. Sergijenko, R. Durrer and V. Pelykh, arXiv:1312.6579 [astro-ph.CO].
 - [48] P. Creminelli, G. D’Amico, J. Norena and F. Vernizzi, *JCAP* **0902** (2009) 018 [arXiv:0811.0827 [astro-ph]].